

# Crystallization kinetics of bulk amorphous Se-Te-Sn system

G. KAUR, T. KOMATSU

*Department of Physics, Faculty of Science, Osaka City University, Osaka 558, Japan*  
*E-mail: bakshi@sci.osaka-cu.ac.jp*

R. THANGARAJ

*Department of Applied Physics, Guru Nanak Dev University, Amritsar, Punjab, India*

In the present work crystallization kinetics of the amorphous  $\text{Se}_{80-x}\text{Te}_{20}\text{Sn}_x$  ( $0 \leq x \leq 9$ ) system have been investigated using Differential Scanning Calorimetry. From the heating rate dependence of the glass transition temperature and the crystallization temperature the activation energy for the glass transition and that for crystallization have been determined using the Kissingers equation and Matusitas equation for non-isothermal crystallization of materials. The effect of addition of Sn to the Se-Te system on the dimensionality of crystal growth has been investigated. An increase in the glass transition temperature with increase in Sn content suggests that Sn plays a role in cross-linking the already existing Se-Te chains which causes an increase in the thermal stability of the material. © 2000 Kluwer Academic Publishers

## 1. Introduction

Chalcogenide glasses are interesting candidates for reversible phase change optical recording devices [1–3]. In the present work a systematic investigation of the crystallization kinetics of amorphous  $\text{Se}_{80-x}\text{Te}_{20}\text{Sn}_x$  ( $0 \leq x \leq 9$ ) system has been made in order to view the suitability of the material for the above applications. The thermal stability and crystallization kinetics have been reported for the Se-Te-Sn system for different Se:Sn ratios. Calorimetric studies were made under non-isothermal conditions at different heating rates. From the heating rate dependence of  $T_g$  and  $T_p$  the activation energies for glass transition and crystallization have been evaluated.

## 2. Experimental procedure

Bulk samples of the  $\text{Se}_{80-x}\text{Te}_{20}\text{Sn}_x$  ( $0 \leq x \leq 9$ ) were prepared by the melt quenching technique. Appropriate amounts of 5 N purity elements were sealed off in quartz ampoules (4 mm diameter) and placed in the furnace at a temperature of 650 °C for 48 hours. The furnace was constantly rocked to ensure a homogeneous mixing of the constituents. The melt was then rapidly quenched in ice water. Quenched samples were removed from the ampoules by dissolving the ampoule in a mixture of  $\text{HF} + \text{H}_2\text{O}_2$  for about 48 hours. Amorphous nature of the samples was ensured by the absence of any sharp peaks in the X-ray diffractograms. Differential Scanning Calorimetry (DSC) measurements were made using a DSC3300, MacScience instrument. DSC thermograms for various compositions of the samples were obtained at different heating rates (5–20 °C/min.) in the temperature range 20–350 °C in order to scan the sam-

ples through their  $T_g$  (glass transition),  $T_p$  (peak crystallization) and  $T_m$  (melting point). The samples (9–10 mg) in powder form were placed in standard platinum pans and scanned over a temperature range of 330 °C.  $T_g$  was taken as the temperature corresponding to the intersection of the two linear portions adjoining the transition elbow in the DSC traces.  $T_c$  is the temperature corresponding to the onset of crystallization. The fraction  $X$  crystallized at a temperature  $T$  is given  $X = A_T/A$  where  $A$  is the total area of the exotherm between  $T_c$  where the crystallization just begins and the temperature  $T_1$  where the crystallization is completed.  $A_T$  is the area between  $T_c$  and  $T$ .

## 3. Results and discussion

### 3.1. Compositional dependence of $T_g$ , $T_p$ , $E_t$ , $E_c$ and dimensionality of crystal growth

DSC curves for  $\text{Se}_{78}\text{Te}_{20}\text{Sn}_2$  are shown in Fig. 1. It can be seen that the  $T_g$  and  $T_p$  of the samples shift to higher temperature with the increase in heating rate. Similar trend is also observed for all the other samples. All the samples show a single glass transition temperature and a single crystallization peak. The variation in the glass transition temperature with composition for the  $\text{Se}_{80-x}\text{Te}_{20}\text{Sn}_x$  ( $0 \leq x \leq 9$ ) system is shown in Fig. 2. It can be seen that the  $T_g$  increases consistently with the increase in Sn concentration at all the heating rates. This indicates that the addition of Sn to the Se-Te system crosslinks the already existing Se-Te chains thus causing an increase in the chain length and hence a more rigid structure resulting in an increase in the  $T_g$  of the material. However the peak crystallization

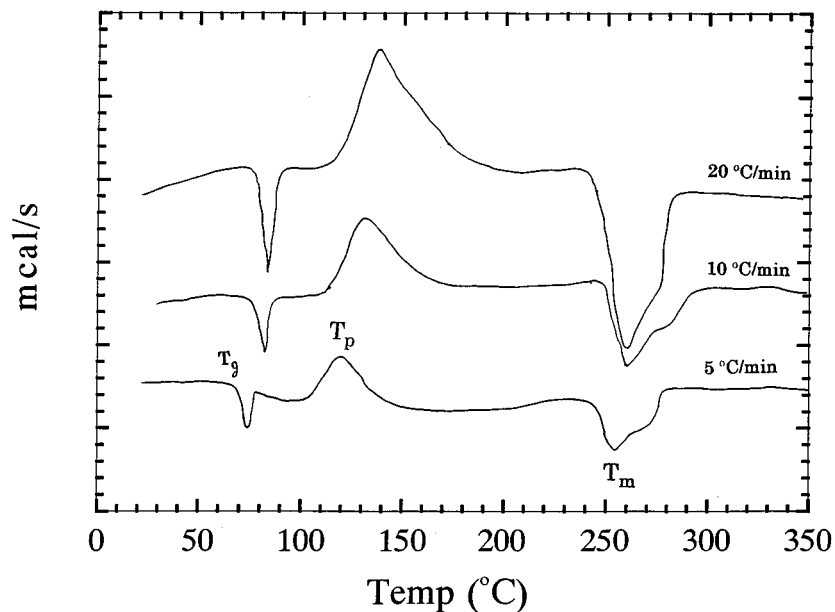


Figure 1 DSC thermograms for  $\text{Se}_{78}\text{Te}_{20}\text{Sn}_2$  at different heating rates showing the glass transition temperature, the peak crystallization temperature and the melting point.

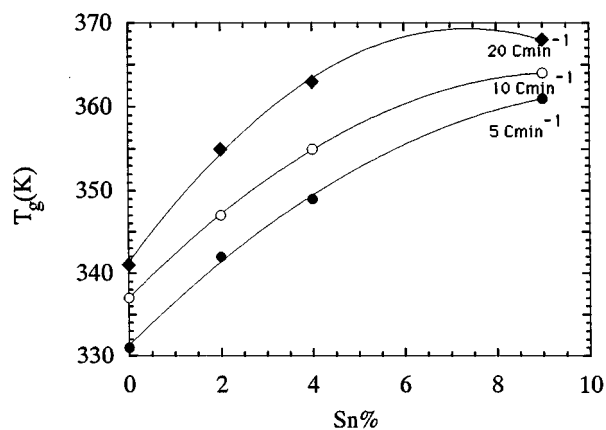


Figure 2 Variation of  $T_g$  with composition for bulk amorphous  $\text{Se}_{80-x}\text{Te}_{20}\text{Sn}_x$  at different heating rates.

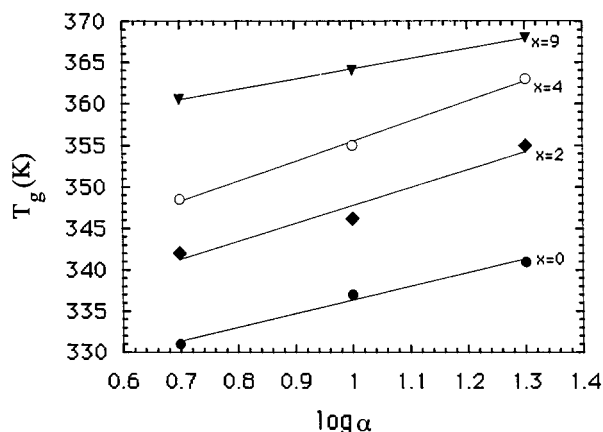


Figure 4  $T_g$  versus  $\log \alpha$  for  $\text{Se}_{80-x}\text{Te}_{20}\text{Sn}_x$  system.

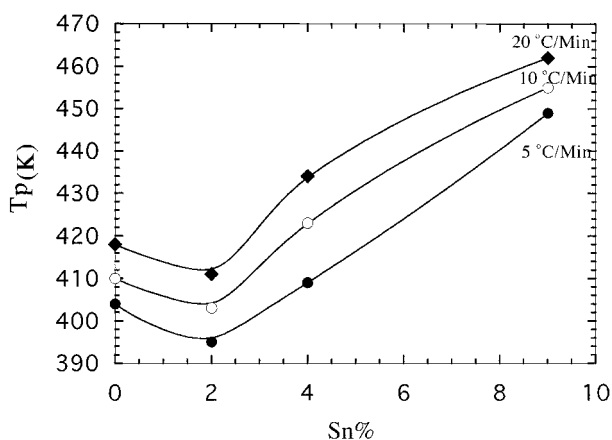


Figure 3 Variation of  $T_p$  with composition for bulk amorphous  $\text{Se}_{80-x}\text{Te}_{20}\text{Sn}_x$  at different heating rates.

temperature shows a slight initial decrease for  $\text{Sn} = 2$  at% and then increases for  $\text{Sn} > 2$  at% as shown in Fig. 3. The melting point is found to increase with the increase in Sn content.

The empirical relation [4]  $T_g = A + B \log \alpha$  where  $A$  and  $B$  are constant, holds good for all the samples.

Plots of  $T_g$  versus  $\log \alpha$  are shown in Fig. 4. The value of  $B$  is found to vary from 12–24 for different samples (Table I). A change in the value of  $B$  indicates structural changes taking place in the samples with the change in composition [4].

The activation energy for glass transition  $E_t$  is calculated using Kissinger's formula [5]

$$\ln\left(\frac{T_g^2}{\alpha}\right) + \text{constant} = \frac{E_t}{RT_g} \quad (1)$$

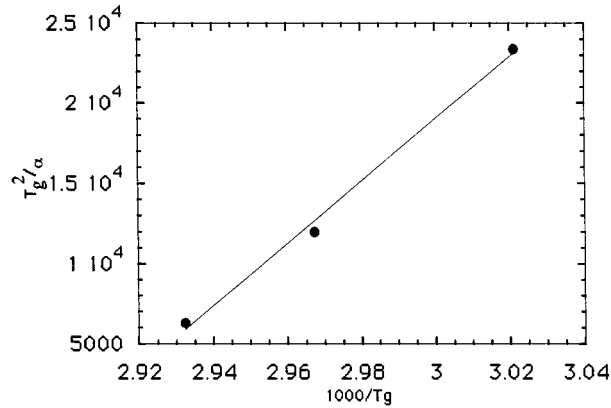
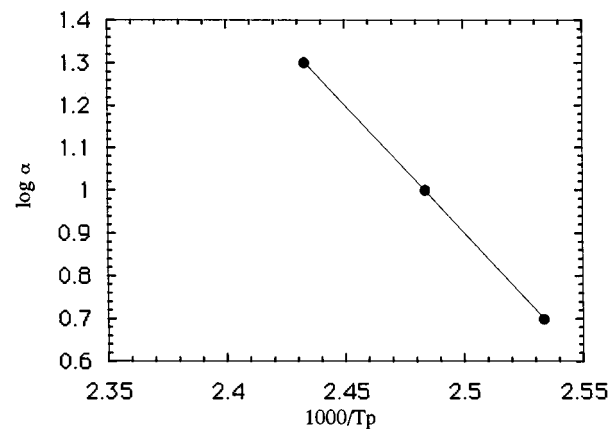
plots of  $\ln(T_g^2/\alpha)$  versus  $1000/T_g$  are found to be linear as seen in Fig. 5. A linear behaviour has been observed for all the samples. Values of  $E_t$  obtained from the graph are listed in Table I. The activation energy for glass transition is found to vary from 23 to 26 Kcal/mol with the addition of Sn.

The activation energy for crystallization  $E_c$  has been obtained using the modified Kissinger equation [6, 7]

$$\ln\left(\frac{\alpha^n}{T_p^2}\right) = -\frac{mE_c}{RT_p} + \ln k \quad (2)$$

TABLE I Parameters determined from the heating rate data on  $\text{Se}_{80-x}\text{Te}_{20}\text{Sn}_x$  samples

Sample	$B$	$E_t$ (Kcal/mol)	$mE_c/n$ (Kcal/mol)	$n$	$m$	$E_c$ (Kcal/mol)	$mE_c$ (Kcal/mol)	$E_c$ (Kcal/mol)
$\text{Se}_{80}\text{Te}_{20}$	14.28	23.98	32.90	4.03	3	43.86	91.25	30.41
$\text{Se}_{78}\text{Te}_{20}\text{Sn}_2$	24	23.10	27.30	2.02	1	54.60	65.86	65.86
$\text{Se}_{76}\text{Te}_{20}\text{Sn}_4$	22	24.17	28.06	2.16	1	56.12	66.97	66.97
$\text{Se}_{71}\text{Te}_{20}\text{Sn}_9$	12	26.34	43.78	2.11	1	87.56	96.44	96.44

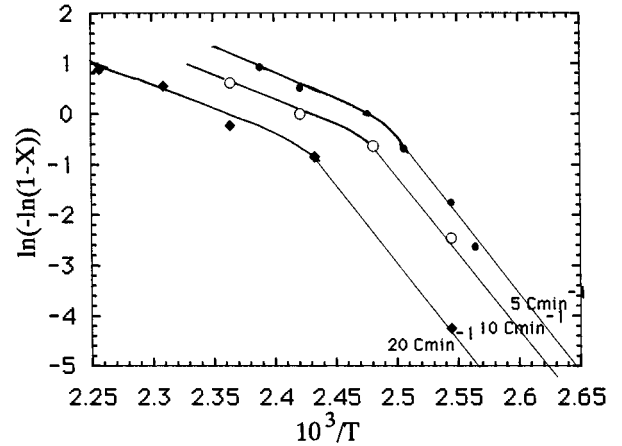

 Figure 5  $\text{Log } T_g^2/\alpha$  versus  $10^3/T_g$  for  $\text{Se}_{78}\text{Te}_{20}\text{Sn}_2$ .

 Figure 6  $\text{Log } \alpha$  versus  $10^3/T_p$  for  $\text{Se}_{78}\text{Te}_{20}\text{Sn}_2$ .

where  $k$  is a constant containing factors depending on the thermal history of the samples,  $n$  and  $m$  are constants having values between 1 and 4 depending on the morphology of growth. The value of  $mE_c/n$  was determined from the slope of  $\ln \alpha$  versus  $1000/T_p$  curves as shown in Fig. 6. The values of  $mE_c/n$  are listed in Table I.

According to Matusita *et al.* [8] for non-isothermal crystallization

$$\ln[-\ln(1-X)] = -n \ln \alpha - 1.052 \frac{mE_c}{RT} + \text{constant} \quad (3)$$

where  $X$  is the volume fraction of crystals precipitated in the glass heated at uniform rate,  $E_c$  is the activation energy for crystallization and  $R$  is the gas constant. The value of  $n$  is obtained from the slope of  $\ln(-\ln(1-X))$  versus  $\ln \alpha$  curve. The value of  $m$  is taken to be  $n - 1$  since no prior heat treatment was given to the samples before the thermal analysis runs.


 Figure 7  $\ln(-\ln(1-X))$  versus  $10^3/T$  for  $\text{Se}_{78}\text{Te}_{20}\text{Sn}_2$  at different heating rates.

It can be seen from the values of  $n$  and  $m$  in Table I that the mechanism of crystal growth changes with the addition of Sn to the Se-Te system. For the  $\text{Se}_{80}\text{Te}_{20}$  sample without Sn,  $n = 4$  which gives  $m = 3$  suggesting bulk nucleation with three dimensional growth. However with the addition of Sn the value of  $n$  becomes 2 and  $m = 1$  which suggests bulk nucleation with one dimensional growth to be the dominant crystallization mechanism. The values of  $E_c$  evaluated using these values of  $m$  and  $n$  are given in Table I column 7. The value of  $mE_c$  (Table I) is obtained from the slope of the  $\ln(-\ln(1-X))$  versus  $1000/T$  curve (Fig. 7). The curve is a straight line for most of the temperature range but shows a break at higher temperatures which is attributed to the saturation of nucleation sites in the final stages of crystallization [9] or to the restriction of crystal growth by the small size of the particles [10]. The analysis is restricted to the initial linear region extending over a larger range.  $E_c$  is again obtained using the value of  $m$  and  $mE_c$ . These values are listed in Table I column 9. The value of  $E_c$  is found to decrease with the addition of a small amount of Sn ( $x = 2$  at%) to the SeTe system indicating an increase in the speed of crystallization which is also consistent with an initial decrease in the  $T_p$  of the sample (Fig. 3). However with the increase in Sn content ( $x \geq 4$  at%) the speed of crystallization decreases resulting in an increase in the activation energy for crystallization.

### 3.2. Thermal stability and the ease of glass formation

Since there is no absolute criterion to parametrize the glass formation the empirical parameters extensively used for its quantitative characterization have been

TABLE II Glass forming tendency of the Se-Te-Sn system at 10 C/min

Sample	$T_g$	$T_c$	$T_m$	$T_c - T_g$	$T_m - T_c$	$K_{gl}$	$T_{rg}$
Se <sub>80</sub> Te <sub>20</sub>	337	402	521	65	119	0.54	0.65
Se <sub>78</sub> Te <sub>20</sub> Sn <sub>2</sub>	346	384	530	37	147	0.25	0.65
Se <sub>76</sub> Te <sub>20</sub> Sn <sub>4</sub>	355	438	533	83	95	0.87	0.66
Se <sub>71</sub> Te <sub>20</sub> Sn <sub>9</sub>	364	443	540	79	97	0.82	0.67

evaluated. The thermal stability is determined from Hrubys parameter  $K_{gl}$  given by [11]

$$K_{gl} = \frac{(T_c - T_g)}{(T_m - T_c)} \quad (4)$$

The values for different compositions vary from 0.25 to 0.87 and are listed in Table II. The ease of glass formation is determined by calculating the reduced glass transition temperature  $T_{rg} = T_g/T_m$  listed in Table II. The value of  $T_{rg}$  is found to be of the order of 2/3 for all the samples thus indicating good glass forming tendency [12] for all the compositions of the material.

#### 4. Conclusion

The effect of addition of Sn to the SeTe system on the crystallization kinetics and thermal stability of the material has been investigated. It is found that the glass transition temperature increases with the increase in Sn content indicating a crosslinking of the SeTe chains with the addition of Sn. The crystallization mechanism is found to change from bulk nucleation in three dimensions for the sample containing no Sn to bulk nucleation in one dimension for the samples containing Sn. All the samples show a good glass forming tendency. The speed of crystallization is maximum for the sample contain-

ing Sn = 2 at% and decreases with further increase in Sn content suggesting that the sample containing Sn = 2 at% is best suited for application to reversible phase change optical recording.

#### Acknowledgement

The authors gratefully acknowledge the help rendered by Dr. Masuda, Deptt. of Geology, Osaka City University, in taking the DSC data. One of the authors Gurinder Kaur is thankful to the Council of Scientific and Industrial Research (Pool Scheme) for providing the financial assistance during the preparation of the samples at Guru Nanak Dev University, Amritsar, India.

#### References

1. Z. L. MAO, H. CHEN and AI-IHEN JUNG, *J. Appl. Phys.* **78**(4) (1995) 2338.
2. R. CHIBA, H. YAMAZAKI, S. YAGI and S. FUJIMORI, *Jpn. J. Appl. Phys.* **32** (1993) 834.
3. MIN SZUKWEI, YANG HANMEI and ZHANG XIAOWEI, *J. Non Cryst. Solids* **112** (1989) 204.
4. M. LASOCKA, *Mater. Sci. Engng.* **23** (1976) 173.
5. H. E. KISSINGER, *J. Res. Nat. Bur. Stand.* **57** (1956) 217.
6. K. MATUSITA and S. SAKKA, *Phys. Chem. Glasses* **20** (1979) 81.
7. D. R. MACFARLANE, M. MATECKI and M. POULAIN, *J. Non Cryst. Solids* **64** (1984) 351.
8. K. MATUSITA, T. KONATSU and R. YOKOTA, *J. Mater. Sci.* **19** (1984) 291.
9. J. COLEMENERO and J. M. BANDARIAN, *J. Non Cryst. Solids* **30** (1978) 263.
10. R. F. SPEYER and S. H. RISBUD, *Phys. Chem. Glasses* **24** (1983) 26.
11. A. HRUBY, *Czech J. Phys. B* **22** (1972) 1187.

Received 28 January

and accepted 11 August 1999